THE JOURNAL OF PHYSICAL CHEMISTRY C

Article

pubs.acs.org/JPCC

Electrochemical Tuning of Localized Surface Plasmon Resonance in Copper Chalcogenide Nanocrystals

Victoria Benavente Llorente,[†,‡] Volodymyr M. Dzhagan,[§] Nikolai Gaponik,[‡] Rodrigo A. Iglesias,[†] Dietrich R. T. Zahn,[§] and Vladimir Lesnyak*[,‡]

[†]INFIQC CONICET, Departamento de Fisicoquímica, Facultad de Ciencias Químicas, Universidad Nacional de Córdoba, Pabellón Argentina Ala 1 piso 2, 5000 Córdoba, Argentina

[‡]Physical Chemistry and Center for Advancing Electronics Dresden (cfAED), TU Dresden, Bergstrasse 66b, 01062 Dresden, Germany

[§]Semiconductor Physics, Chemnitz University of Technology, 09107 Chemnitz, Germany

ABSTRACT: In this work, we developed a method to study *in situ* the optical properties of $Cu_{2-x}Se$ and CuS nanocrystals upon electrochemical reduction and oxidation. Both these materials possess a strong localized surface plasmon resonance (LSPR) in the near-infrared region. First, the nanoparticles were embedded into a transparent film made of a perfluorinated sulfonic-acid copolymer Nafion deposited onto an ITO-coated glass. This substrate was employed as a working electrode for chronoamperometry and cyclic voltammetry measurements directly in a transparent cell allowing for simultaneous acquisition of absorption spectra of the system upon its charging/discharging. We observed that LSPR of the $Cu_{2-x}Se$ NCs can be well-controlled and tuned in a wide range simply by potentiostatic potential switching. Starting with an intensive plasmon of the initial as-synthesized $Cu_{2-x}Se$ NCs we were able to completely damp it via reduction (electron injection). Moreover, this electrochemical tuning was demonstrated to be reversible by subsequent oxidation (extracting electrons from the system). At the same time, CuS NCs did not exhibit such prominent LSPR modulation upon the same experimental conditions due to their more metallic-like electronic structure. Hence, our findings demonstrate for the first time a reversible tuning of the LSPR of copper chalcogenide NCs without any chemical or structural modification. Such a wide LSPR tunability is of paramount importance, for example in applications of these materials in photovoltaics to amplify light absorption, in systems involving plasmon−exciton interactions to controllably quench/enhance light emission, and in electrochromic devices to control their transmittance.

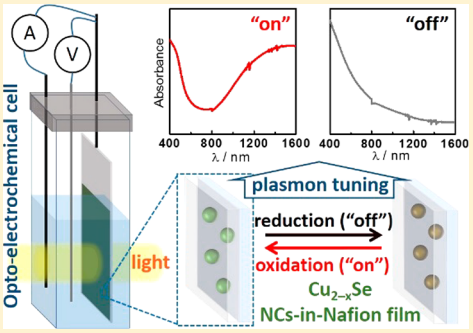

INTRODUCTION

Recent years of intensive research on colloidal semiconductor nanocrystals (NCs) prepared by wet chemical approaches have revealed one more phenomenon of these materials, namely their ability to sustain a localized surface plasmon resonance (LSPR) similar to noble metal nanoparticles.[1−6] This feature together with well-known unique quantum confinement effects observed in nanosized semiconductors provide an additional tool to tune and harness their optoelectronic properties. A new member has been added to the family of plasmonic nanomaterials in 2009, when Zhao et al. interpreted the optical absorption of $Cu_{2-x}S$ nanoparticles in the near-infrared region (NIR) as a LSPR,[7] later confirmed by the group of Alivisatos.[8] Unlike in noble metal nanoparticles, where a plasmon is generated by the collective oscillation of electrons interacting with visible light, in copper chalcogenides free charge carriers are holes. These holes can be either associated with copper vacancies in substoichiometric $Cu_{2-x}S$,[9,10] $Cu_{2-x}Se$,[10−13] and $Cu_{2-x}Te$[10,14] or rather delocalized over the entire valence bands in covellite-type CuS[15,16] and klockmannite-type CuSe[17] NCs. Substoichiometric copper chalcogenides are also called self-doped or degeneratively doped semiconductors owing to their ability to uphold a large number of copper vacancies in their crystal structure. The most recent and comprehensive review on plasmonic doped semiconductor NCs was published by Kriegel and coauthors.[6]

Easy self-doping makes possible the fine-tuning of the position and relative intensity of the LSPR band of these NCs by the variation of the number of vacancies, hence the number of charge carriers associated with these vacancies. This tuning is commonly achieved by a chemical treatment of the NCs with oxidizing or reducing agents.[3,9−11,18] Here, the first process (oxidation) results in the formation of Cu vacancies and the raise of the LSPR with its gradual shift to higher energies (shorter wavelengths), while the latter (reduction) extinguishes free holes leading to the shift of the plasmon to lower energies (longer wavelengths) and its complete damping. By exposing a Cu_2Se NC film to air, Riha et al. demonstrated a 3000-fold increase of its conductivity accompanied by changes from semiconducting to ohmic behavior.[19] First reversible tuning of

Received: June 1, 2017
Revised: July 20, 2017
Published: July 24, 2017

DOI: 10.1021/acs.jpcc.7b05334
J. Phys. Chem. C 2017, 121, 18244−18253

the LSPR was demonstrated by Dorfs et al. on $Cu_{2-x}Se$ NCs treated either with $(NH_4)_2Ce(NO_3)_6$ (oxidant) or simply exposed to air to induce slow oxidation, or with Cu(I)-$(CH_3CN)_4PF_6$ (reductant) in solution.[11] In this case tetrakis-(acetonitrile)copper(I) hexafluorophosphate acts as a source of copper ions which can fill the vacancies in oxidized NCs and thus reestablish their stoichiometry. Up to now it is not very clear what exactly happens when other reducing agents which do not contain any copper are used, such as diisobutylaluminum hydride[10] or lithium triethylborohydride.[20] For the oxidation process, Kriegel et al. proposed that copper species form a thin layer at the NC surface either in the form of CuO or as a monolayer of Cu(II) atoms bound to surface ligands.[10] In a similar oxidation of Cu_2Se NCs in solution Dorfs et al. observed the formation of small CuO nanoparticles from Cu^{2+} species ejected out of the NCs.[11] In this scenario the addition of a reducing agent should lead to the reduction of Cu^{2+} and following reinsertion of the forming Cu^+ ions back into the copper chalcogenide particles.

Among other factors affecting the LSPR of copper chalcogenide NCs are their size[8,10] and shape,[21−23] as well as dielectric properties of the surrounding medium,[8,24] similar to noble metal contenders. For example, the LSPR of $Cu_{2-x}S$ shifts to higher energies when the size of the NCs increases.[8,10] Postsynthetic ligand exchange on copper chalcogenide NCs can also change the LSPR energy position.[14,24,25] In this way, the attachment of electron accepting or donating ligands to the surface of $Cu_{2-x}Se$ NCs was reported to result in a LSPR shift over approximately 200 nm due to the change in carrier density.[25]

As follows from the above summarized literature, most of the approaches to postsynthetic LSPR tuning in copper chalcogenide NCs involve their chemical oxidation and/or reduction in solution and thus variation of their composition (stoichiometry). At the same time, to the best of our knowledge there are no published studies of nonchemical impact on the NCs via direct injection/withdrawal of charge carriers and its influence on their optical properties. Therefore, in this work, we present a spectroelectrochemical characterization of plasmonic $Cu_{2-x}Se$ and CuS NCs. In our approach we combine *in situ* optical absorption spectroscopy with chronoamperometry and cyclic voltammetry methods in order to get insight into the processes responsible for the LSPR modulation in these two types of NCs. By simultaneous recording absorption spectra and the electric potential of the system we avoid possible rearrangements of the crystal structure, which may happen on a prolonged time scale, and thus exclude additional processes which might affect the plasmon response. Electrochemistry provides powerful approaches to probe semiconductor nanoparticles, although it has been mostly employed to investigate "classical" cadmium chalcogenide-based quantum dots.[26−31] Such electrochemical method as cyclic voltammetry is especially useful in studying redox processes in a wide range of different compounds.[32] Our findings indicate that the two chosen types of nanoparticles ($Cu_{2-x}Se$ and CuS NCs) behave differently upon similar experimental conditions of the measurements. While substoichiometric $Cu_{2-x}Se$ NCs exhibit a broad modulation of the LSPR which can be reversed simply by changing the potential in the system, stoichiometric CuS NCs are much more rigid and practically do not display any tuning of their absorption spectra. Thus, despite both materials contain Cu^+ ions (here we note that although CuS appears to contain Cu^{2+} ions according to its stoichiometry, in fact it is built of Cu^+ ions and sulfur having an average oxidation state close to −1, an established fact which is often overlooked)[15] which are prone to oxidation, the tunability of the LSPR is achievable only with $Cu_{2-x}Se$ NCs. The results of our study open up new perspectives for the application of the NIR plasmonic self-doped copper chalcogenide NCs in solar cells combining them with materials like Cu−Zn−Sn−S(Se) or PbS quantum dots to amplify light absorption of the system. Moreover, these plasmonic NCs can be integrated in structures involving plasmon-exciton interactions and local field enhancements to modulate their light emission properties,[33−35] or in electrochromic light filtering devices to manipulate their transmittance, *etc.*

EXPERIMENTAL SECTION

Materials. Copper(II) acetylacetonate ($Cu(acac)_2$, 97%), CuCl (≥97%), Se powder (≥99%), S powder (99,98%), 1-dodecanethiol (≥98%), oleylamine (OlAm, 80%−90%), octadecene (ODE, 90%), Nafion DE 520 (5 wt % in a mixture of lower aliphatic alcohols and water, contains 45% of water), tetrachloroethylene (TCE, ≥ 99%), tetrabutylammonium hexafluorophosphate (TBAHFP, ≥ 98%), anhydrous dichloromethane (DCM, ≥ 98%), acetonitrile, 2-propanol, acetone, methanol, and toluene were purchased from Sigma-Aldrich. Chemicals were used without any further purification.

Synthesis of $Cu_{2-x}Se$ Nanocrystals. The synthesis of $Cu_{2-x}Se$ NCs was performed according to the recipe published in ref 12 using a standard Schlenk line technique.

Synthesis of CuS Nanocrystals. The synthesis of covellite CuS NCs was performed according to a recipe by Xie et al.[16] with some modifications. First, a S-precursor was prepared by dissolving 32 mg (1 mmol) of S powder in 2.5 mL of ODE and 2.5 mL of OlAm by degassing under vacuum at approximately 60 °C for 0.5−1 h with subsequent heating to 100 °C upon vigorous stirring under nitrogen gas protection. In parallel, a Cu-precursor was prepared. 2.5 mL of ODE and 2.5 mL of OlAm were degassed under vacuum at approximately 60 °C for 0.5−1 h in a 25 mL three-neck round-bottom flask. Afterward this flask was filled with nitrogen and 50 mg (0.5 mmol) of CuCl were quickly added in inert gas flow to avoid oxidation of the salt. The mixture turned greenish and was heated to 200 °C whereupon turning colorless. At this temperature the S-precursor heated to 100 °C was quickly injected from a syringe upon vigorous stirring. After the injection, the reaction mixture turned dark-green and was kept at 200 °C for 5 min. After quenching the reaction by cooling down to room temperature, the mixture was centrifuged at 5000 rpm for 20 min. The clear and almost colorless supernatant was discarded and the precipitate containing CuS NCs was redispersed in 3 mL of toluene. The NCs were washed by additional reprecipitation by addition of 1−2 mL of methanol with subsequent centrifugation and redispersion in 1−2 mL of toluene.

UV−Vis−NIR Spectroscopy. Absorbance spectra of $Cu_{2-x}Se$ and CuS NCs dispersed in TCE were recorded in 1 cm path length quartz cuvettes using a Cary 5000 (Varian) UV−vis−NIR spectrophotometer.

Transmission Electron Microscopy (TEM). Samples were prepared by dropping diluted NC suspensions onto carbon coated 200 mesh copper grids with subsequent evaporation of the solvent. Conventional TEM imaging was performed on a TECNAI F30 microscope equipped with a field emitter operating at 300 kV accelerating voltage.

DOI: 10.1021/acs.jpcc.7b05334
J. Phys. Chem. C 2017, 121, 18244−18253

Cyclic Voltammetry Measurements. Cyclic voltammograms were recorded on an Autolab potentiostat, using glassy carbon disks as the working electrode (area ca. 0.07 cm^2), a Pt wire as a counter electrode, and a Ag wire as a pseudoreference electrode.[36] The working electrodes were polished, cleaned, and dried before dropcasting the NCs. In one set of measurements we deposited NCs directly on top of the electrodes by dropcasting approximately 2 μL of a diluted stock solution of the NCs with subsequent drying. Alternatively, we characterized the NCs embedded in Nafion. In this case, 50 μL of the original stock solution of Nafion were mixed with approximately 100 μL of the NC stock solution in toluene upon ultrasonication. This freshly prepared mixture was simply drop-casted on a glassy carbon electrode with subsequent evaporation of the solvents. TBAHFP dissolved in acetonitrile (10 mM) was employed as a supporting electrolyte in the measurements of bare NCs and 10 mM TBAHFP solution in DCM was used to characterize the mixed samples. The electrochemical cell containing electrolyte was thoroughly deoxygenated by purging with nitrogen (or argon) for approximately 15−20 min prior to inserting the working electrode and starting the measurements. The scan rate was set to 25 $mV{\cdot}s^{-1}$ by a potentiostat μautolab type III.

Spectroelectrochemical Measurements. A three electrode cell built inside of a 1 cm path length quartz cuvette was employed for the measurements. Pt and Ag wires were used as a counter and a pseudoreference electrode, respectively. Working electrodes were prepared as follows: ITO-coated glasses were cleaned with 2-propanol, acetone, ethanol, and Milli-Q water by ultrasonication for 5 min in each solvent. 100 μL of the $Cu_{2-x}Se$ or CuS NC solutions prepared as described above were mixed with 50 μL of Nafion during 10 min by ultrasonication. These mixtures were drop-casted on the ITO substrates and left for drying forming a continuous film. The electrolyte, 0.1 M TBAHFP in DCM, was purged with argon for several minutes prior to measurements. After assembling the cell and connecting all electrodes to a potentiostat μautolab type III, it was introduced into a sample holder of a Cary 5000 (Varian) UV−vis−NIR spectrophotometer for simultaneous optical and electrochemical characterization. The scheme of the setup is presented in Figure 1. For all spectroelectrochemical measurements the acquisition of absorption spectra was performed in the 400−2000 nm range with the scan rate of 2000 $nm{\cdot}min^{-1}$.

Photoelectron X-ray Spectroscopy (XPS). XPS was performed with an ESCALAB 250Xi X-ray Photoelectron Spectrometer Microprobe (Thermo Scientific). The spectral resolution of 0.5 eV was provided by a monochromatized Al Kα ($h\nu$ = 1486.6 eV) X-ray source. To prevent possible charging of the samples, a flooding of the sample with low kinetic energy electrons was used. Spectra deconvolution and quantification were performed using the Avantage Data System (Thermo Scientific). For the XPS study we used as-prepared $Cu_{2-x}Se$ NCs-in-Nafion films deposited onto ITO-coated glass (working electrode) before and after its reduction (before and after the plasmon damping) together with two reference samples, the as-prepared $Cu_{2-x}Se$ NCs deposited directly from their dispersion and a pure Nafion film. For the calibration of energies of elements analyzed we used the position of the C 1s peak corresponding to C−C bond at 484.5 eV as a reference.

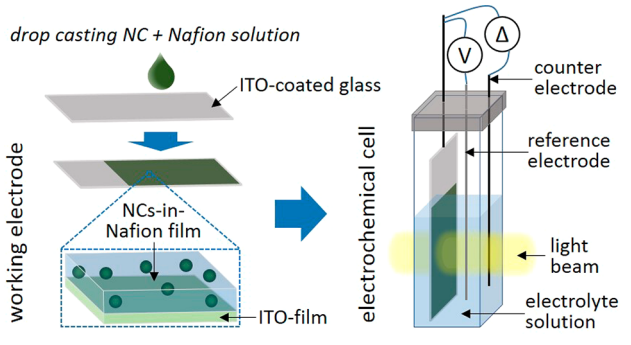

Figure 1. Scheme of the working electrode preparation and electrochemical cell assembly used to measure optical absorbance of the NCs-in-Nafion films in response to electrochemical stimuli *in situ*.

RESULTS AND DISCUSSION

Synthesis of the $Cu_{2-x}Se$ and CuS NCs and Preparation of the NCs-in-Nafion Films. To get insight into the plasmonic features of copper chalcogenide NCs we chose two main materials, i.e., substoichiometric $Cu_{2-x}Se$ particles and stoichiometric covellite CuS nanodisks. Copper selenide NCs can accommodate a large number of Cu vacancies in their crystal structure, which are responsible for their p-doping giving rise to a strong LSPR in the NIR region. In fact, in as-synthesized $Cu_{2-x}Se$ NCs almost one-third of copper atoms is missing ($x \approx 0.6$).[12] Whereas in the case of covellite CuS, which is a stoichiometric compound, the vacancies are absent and holes are delocalized over the entire valence band owing to peculiarities of its structure, resulting in metallic-like properties of this material described in detail by Xie et al.[15] It was demonstrated that the incorporation of Cu^+ ions into these particles results in the rearrangement of the crystal structure with a transformation to the chalcocite phase with a composition close to Cu_2S.[16] Despite these two members of the copper chalcogenide family ($Cu_{2-x}Se$ and CuS NCs) have similar LSPRs with maxima positioned in the range of 1100−1200 nm (see Figure 2), the relation between their crystal structure and electronic (optical) properties is different. Therefore, it is interesting to compare the optical response of these two types of NCs to direct injection/withdrawal of charge carriers without adding any chemical agents to the system.

In order to study simultaneously optical and electrochemical properties of the NCs in one setup we built a cell as shown in Figure 1. In this cell we used an ITO-coated glass as a transparent conducting substrate to deposit nanoparticles. Simple drop-casting of the NCs on the ITO typically led to a detachment of the NC film during electrochemical measurements in an electrolyte solution, as these particles are well soluble in low polar and nonpolar organic solvents, such as DCM and acetonitrile used in our measurements. In addition, direct contact with the electrolyte could affect the optoelectronic properties of the samples. Therefore, in order to fix the NCs on ITO and protect them from the electrolyte we incorporated them into a Nafion film. Nafion is a perfluorosulfonated resin able to conduct protons and is commonly used as a membrane in fuel cells and in electrochemical experiments.[37] The films were prepared by drop-casting a mixture of the NCs in toluene and Nafion dissolved in aliphatic alcohols containing water with subsequent evaporation of the solvents. The obtained $Cu_{2-x}Se$ NCs-in-Nafion and CuS NCs-in-Nafion composite films maintained the greenish color of the as-prepared particles and were stable in DCM. Furthermore, the films also retained the characteristic

DOI: 10.1021/acs.jpcc.7b05334
J. Phys. Chem. C 2017, 121, 18244−18253

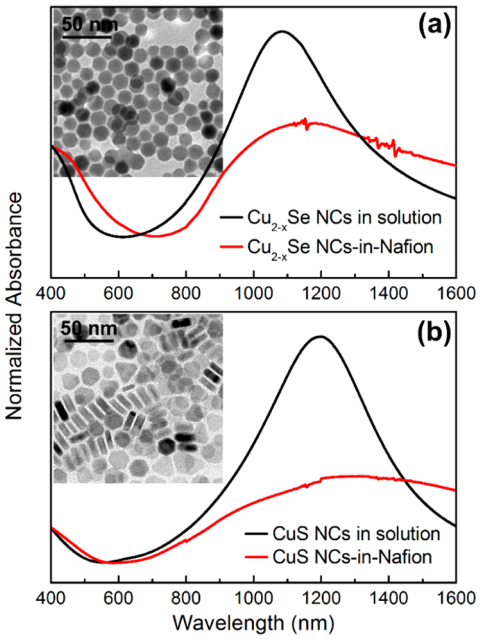

Figure 2. Normalized optical absorption spectra of $Cu_{2-x}Se$ NCs dispersed in TCE and $Cu_{2-x}Se$ NCs-in-Nafion film on ITO immersed in the electrolyte (a). Normalization was based on the equation of the visible parts of the spectra. Absorption spectra of CuS NCs in solution and in the form of the composite (b). Insets are TEM images of corresponding NCs prepared from dispersions.

absorption properties of the original materials in both cases, although the LSPR bands broadened and red-shifted in relation to the NCs in solution (Figure 2). These changes can be attributed to a partial aggregation of the nanoparticles in the toluene-alcohol−water-Nafion mixture, leading to a delocalization of the charge carriers over whole aggregates as well as to an electron donating effect of the functional groups of Nafion.

Electrochemical Investigation of the NCs and the NCs-in-Nafion Films. As a part of electrochemical characterization of the materials we performed voltammetric measurements of the NCs deposited on glassy carbon electrodes starting from open circuit potential (E_{OC}) toward negative potential values and then reverted to positive potential, since the as-synthesized highly vacant $Cu_{2-x}Se$ NCs can be defined as "oxidized" and thus need to be reduced first. The investigation of the $Cu_{2-x}Se$ NCs involved first their immobilization on the surface of an electrode. Even though nanoparticles themselves can be adsorbed nonspecifically on the surface of a glassy carbon electrode, they are not stable during the potential scan. Figure 3a shows a cyclic voltammogram of the $Cu_{2-x}Se$ NCs deposited on a glassy carbon electrode when the potential is swept from E_{OC} toward negative values (reduction), followed by a second scan with positive sweep direction (oxidation) and back to negative potential during the third scan. During the first scan very moderate reduction current is observed in the potential region below 0.4 V. However, as the potential increases during the second scan the pronounced oxidation peak A1 starts to develop; i.e., the number of vacancies rises (x value in $Cu_{2-x}Se$ increases). During the third scan (negative direction, reduction) the vacancies created via the oxidation process can be reduced by two different cathodic processes, A2 and A3 at +0.30 and −0.37 V, respectively. This behavior progressively changes as the potential is swept during several following cycles (not shown in the graph), revealing a continuous dissolution (detachment or decomposition) of the particles. This observation is in accordance with previous reports showing that $Cu_{2-x}Se$ NCs release CuO upon chemical oxidation.

To stabilize the particles in the system they were embedded in a Nafion polymer film deposited on the surface of a glassy carbon electrode. Even though the overall voltammetric behavior is similar to that of the bare NCs, the environmental conditions provided by Nafion encapsulation change the E_{OC} of the electrode (Figure 3b). $Cu_{2-x}Se$ NCs-in-Nafion composite exhibits an E_{OC} located at a potential more positive than the range in which the NCs can be oxidized. Therefore, when the potential sweeps toward negative values (reduction) starting from E_{OC} = 0.60 V, we observe a reduction peak already during

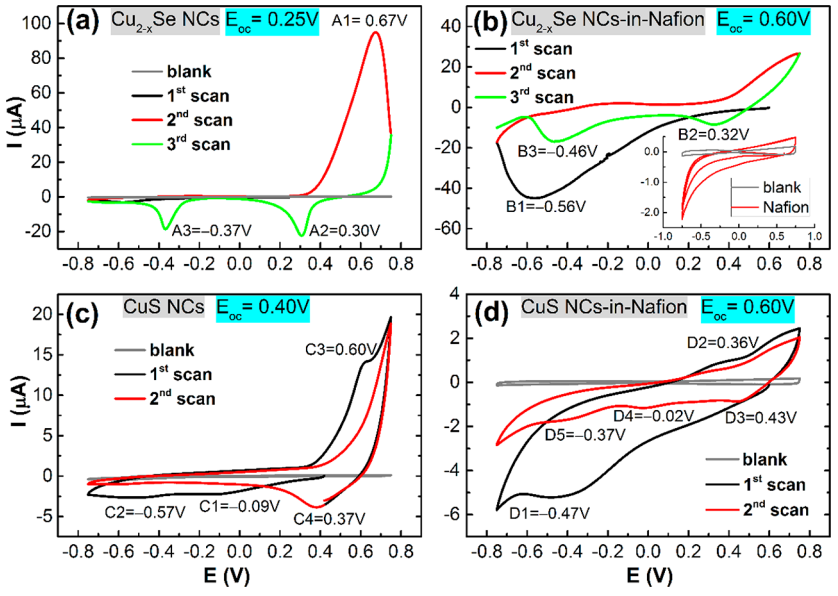

Figure 3. Cyclic voltammograms of $Cu_{2-x}Se$ (a) and CuS (c) NC solutions (scan rate =25 $mV \cdot s^{-1}$), and corresponding NCs-in-Nafion composites (b and d, respectively). Inset in frame b shows magnified voltammograms of the blank and Nafion samples.

DOI: 10.1021/acs.jpcc.7b05334
J. Phys. Chem. C 2017, 121, 18244−18253

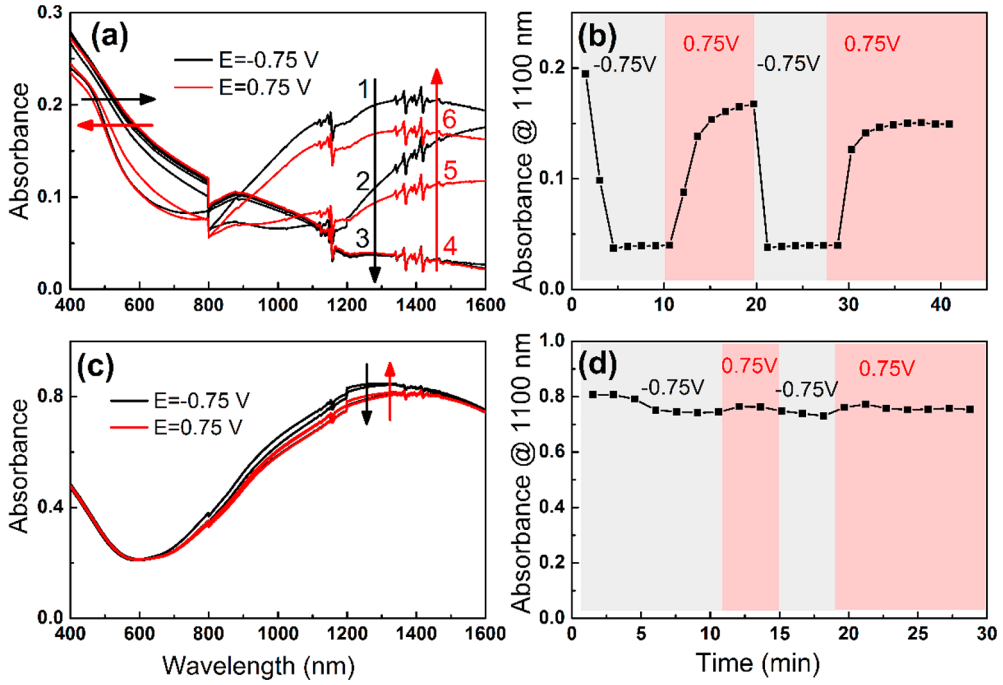

Figure 4. Absorption spectra of $Cu_{2-x}Se$ NCs-in-Nafion (a) and CuS NCs-in-Nafion (c) films recorded *in situ* during their electrochemical reduction and oxidation. Absorbance of these films recorded at λ = 1100 nm by applying consecutive potential steps (b and d). Note that the dips in the absorption spectra at 800 nm in (a) are caused by a detector changeover.

the first scan corresponding to the extinguishing of holes present in the as-synthesized NCs at the beginning of the experiment. Similarly to the bare particles, during the positive (second) scan only one oxidation process (at about 0.60 V) takes place, creating vacancies in the material. It should be noted that the reduction−oxidation of the NCs can be cycled repeatedly when they are embedded in the Nafion film (see below in the Spectroelectrochemical Characterization), which is impossible in the case of the unprotected particles. Thus, by the immobilization of the $Cu_{2-x}Se$ NCs in Nafion, it was possible to address the particles electrochemically in such a way that they can be reduced and oxidized several times avoiding their decomposition and allowed us to use this approach on an optically transparent electrode in order to study the *in situ* modulation of the LSPR by changing the electrochemical potential.

Cyclic voltammetry of CuS NCs revealed two less resolved reduction peaks at −0.09 V (C1) and at −0.57 V (C2) and an oxidation peak at 0.60 V (C3) in the first scan followed by an additional reduction peak at 0.37 V (C4) in the second scan (Figure 3c). Voltammograms of the NCs-in-Nafion composites exhibit remarkable differences from those of the bare particles. Thus, in the first scan of the $Cu_{2-x}Se$ NCs-in-Nafion film we observed only one reduction peak, at −0.56 V (B1). In the second scan two additional reduction peaks at +0.32 V (B2) and at −0.46 V (B3) appeared in the voltammogram. The voltammogram of the CuS NCs-in-Nafion composite exhibited one reduction at −0.47 V (D1) and one oxidation at +0.36 V (D2) signals in the first scan accompanied by three reduction features at +0.43 (D3), −0.02 (D4), and −0.37 V (D5) which were identified in the second scan (Figure 3d).

Comparing the two sets of data, one can notice the difference in the ratio between intensities of reduction and oxidation peaks in bare NCs and those embedded into Nafion. While bare NCs exhibit more pronounced oxidation features, in the voltammograms of the composites the intensities of the reduction signals dominate. Moreover, in the NCs-in-Nafion samples all features are smoothed and positions of the peaks are not well-defined. These observations imply that oxidation processes are more prominent in bare NCs, whereas in the case of the composite samples reduction processes are more pronounced. One can rationalize this behavior taking into account the specific conductivity of Nafion, which selectively transports positively charged species, such as protons, rather than negatively charged electrons or anions.[37] Although the conductivity and transport phenomena in Nafion have been deeply investigated, for example, by the fuel cell community, the underlying mechanisms show a high level of complexity,[38] which makes an exact interpretation of the observed broad electrochemical features literally impossible in the framework of the present study. Nevertheless, the data shown in Figure 3 allowed us to conclude that the NCs embedded in the Nafion matrix appear to be in contact with the working electrode and can be polarized (i.e., charged/discharged) by applying an electrochemical potential.

Spectroelectrochemical Characterization of $Cu_{2-x}Se$ NCs-in-Nafion and CuS NCs-in-Nafion Composite Films. After cyclic voltammetry measurements, which showed that both types of the NCs undergo redox processes, we studied the optical response of the NCs-in-Nafion composite films by applying potential steps of −0.75 and +0.75 V, alternately. We observed that the application of a cathodic (negative) potential to the $Cu_{2-x}Se$ NCs-in-Nafion led to a gradual red shift of the LSPR accompanied by the decrease of its intensity (Figure 4a). Eventually, the LSPR was totally damped. In addition to the plasmon band, the characteristic absorption in the visible region also underwent a gradual red-shift. By reversing the potential to the positive value the LSPR increased gradually and finally recovered to the original value and the spectral shape. The absorption in the visible region also blue-shifted back to its

DOI: 10.1021/acs.jpcc.7b05334
J. Phys. Chem. C 2017, 121, 18244−18253

initial values. This cycle can be repeated several times simply by changing the potential of the working electrode: reduction of the $Cu_{2-x}Se$ NCs-in-Nafion resulted in the damping of the LSPR, while reoxidation led to its recovery (Figure 4b).

Unlike the $Cu_{2-x}Se$ NCs, the application of the same potentials to the CuS NCs-in-Nafion film did not lead to such prominent changes in its absorption spectra and only a slight modulation was achieved (Figure 4c,d). This finding suggests that the absence of copper vacancies in CuS makes the structure less flexible and does not allow for remarkable tuning of the optoelectronic properties, a behavior similar to plasmonic noble metal NCs.[39,40] For example, nanoporous gold films exhibited a remarkable 30% near-infrared transmission change by applying a potential of 0.9 V leading to a corresponding change in average charge carrier density up to 8%.[39] At the same time, charging/discharging a film made of colloidal Au nanoparticles with a size of 60 nm on an ITO-coated glass by sweeping the applied bias from +2.25 to −2.25 V resulted in only 7% change of the peak extinction compared to its initial state at 0 V.[40] In our experiment a small red-shift of the peak was observed at a positive applied bias and a blue-shift and increase in the peak height was observed under negative applied bias. Thus, under the experimental conditions employed it was not possible to alter the concentration of free charge carriers in unique metallic-like covellite structure either by reducing or oxidizing the sample. This is in contrast to recent results obtained by Kalanur and Seo on CuS thin films prepared by chemical bath deposition, in which the authors were able to suppress the LSPR by injecting electrons in the system.[41] In that case, however, the film was in the direct contact with 0.1 M aqueous solution of perchloric acid, which by itself (without polarization) can cause irreversible changes of the film and thus its optical response.

In order to investigate the effect of the electrolyte concentration on the modulation of absorption spectra of the $Cu_{2-x}Se$ NCs-in-Nafion we repeated the experiment using the same potentials but with increasing the TBAHFP concentration for each potential cycle. The changes of the absorption spectra, their amplitude and rate remained basically the same, suggesting that this behavior was independent of the electrolyte concentration (Figure 5a). Hence, this observation implies that $(C_4H_9)_4N^+$ ions do not participate directly in the filling of copper vacancies in the NCs, otherwise one should see a dependence of the spectral modulation rate on the concentration of the electrolyte. To support this assumption we performed additional measurements in the presence of copper or zinc containing molecules, copper acetylacetonate and zinc diethyldithiocarbamate. Both compounds may participate in an overall redox process releasing Cu^+ or Zn^{2+} ions, which can fill copper vacancies in $Cu_{2-x}Se$ NCs dispersed in solution.[12] In our case, however, we did not observe any difference in spectral response of the NCs-in-Nafion film in the presence of both compounds, which suggests that even if these cations are formed in the electrolyte they are not able to reach the nanoparticles embedded in the polymer.

After electrochemical reduction of the sample, the absorption spectra were recorded under open circuit conditions for a certain time. While the reduction of the film led to the damping of the LPSR of the NCs, when the potential was no longer applied, the LPSR intensity started gradually increasing (Figure 5b). When the electrolyte was removed from the cell, the plasmon band continued restoring upon exposure to air. This measurement demonstrates that the LSPR damping by the

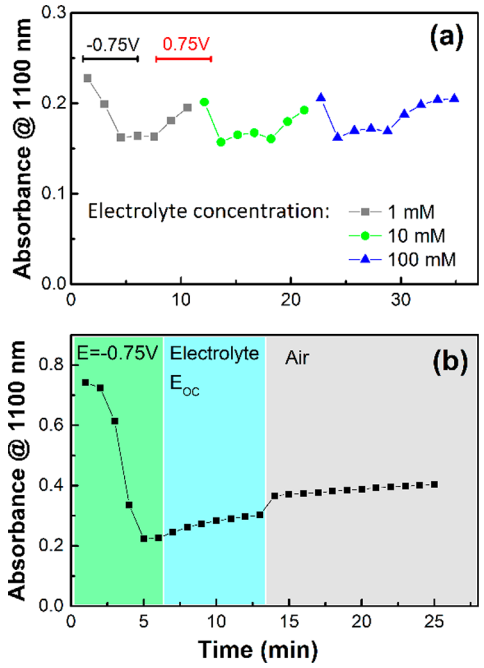

Figure 5. (a) Absorbance recorded at λ = 1100 nm during application of consecutive potential steps on $Cu_{2-x}Se$ NCs-in-Nafion films with different electrolyte concentrations. (b) Absorbance recorded at λ = 1100 nm at three stages: (i) application of the negative potential, (ii) under open circuit conditions, and (iii) after removal of the electrolyte and exposure to air.

electrochemical reduction can be spontaneously and slowly reverted either in the electrolyte or by simple exposure to air resulting in the reoxidation of the $Cu_{2-x}Se$ NCs. The latter is an established way to generate vacancies in the copper chalcogenide NCs both in solution and in the solid state, as mentioned in the introduction.

To detail the picture of the LSPR behavior depending on the applied potential, we combined *in situ* cyclic voltammetry measurements with absorption spectroscopy performed on the $Cu_{2-x}Se$ NCs-in-Nafion composite film. We note that the absorption spectra were recorded during the entire scan, however, only those spectra relevant for the corresponding changes in the voltammogram are shown in Figure 6. Each spectrum in Figure 6a was recorded during a potential interval which is marked on the cyclic voltammogram in Figure 6b by straight lines. Spectrum number 1 was acquired prior to potential cycling. During the scan, we observed that at a potential of about −0.2 V the LSPR maximum already started to shift to longer wavelengths and its intensity began to decrease with complete damping when the potential reached values below −0.6 V (Figure 6). The regeneration of the LSPR started when the potential reached a value over 0.25 V in the reverse scan and was almost completely restored at the positive potential of about 1.0 V. Note that these peaks were not present in the blank sample (ITO-glass slide coated with Nafion). These two features can be directly related to the optical changes, since the damping and regeneration of the LSPR occurred at about these potentials. The results of the *in situ* cyclic voltammetry corroborate well the cyclic voltammogram of bare $Cu_{2-x}Se$ NCs presented in Figure 3a, where the corresponding reduction and oxidation peaks are better resolved. From this curve one can see more clearly, that at a potential below −0.2 V a reduction process starts and reaches

DOI: 10.1021/acs.jpcc.7b05334
J. Phys. Chem. C 2017, 121, 18244−18253

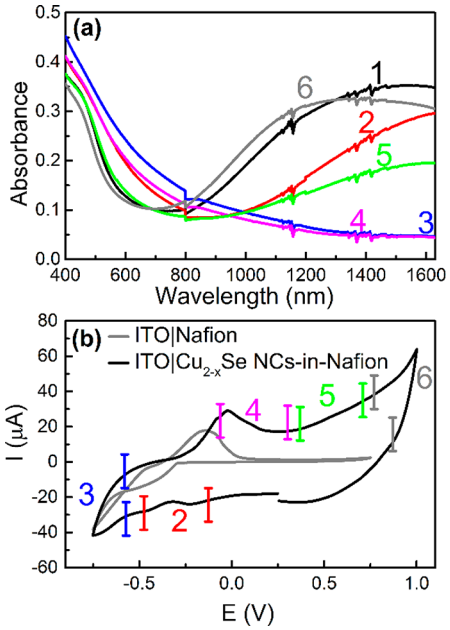

Figure 6. (a) Absorption spectra of the $Cu_{2-x}Se$ NCs-in-Nafion film recorded during cyclic voltammetry measurements. (b) Cyclic voltammograms of the composite and the blank sample (ITO-glass slide coated with Nafion). Electrolyte: TBAHPF in DCM. Scan rate =5 $mV{\cdot}s^{-1}$.

its peak intensity at −0.30 V (A2) with the next less prominent peak A3 at −0.37 V corresponding to the complete disappearance of the plasmon band in the absorption spectrum 3 in Figure 6a. After reversing the potential to a positive direction the LSPR gradually intensifies and shifts to shorter wavelengths (spectra 4−6) reaching its maximum at a potential above 0.6 V, corresponding to the oxidation peak A1 at 0.67 V in Figure 3a. Therefore, playing with the potential applied to the working electrode in the range between −0.6 and approximately 0.7 we can reversibly tune the plasmon from its maximal intensity (turn on) down to complete damping (turn off). A more fine control of the LSPR, which can be cycled several times from turn on to turn off states, was achieved by applying a lower scan rate of 1 $mV{\cdot}s^{-1}$.

XPS Characterization of the $Cu_{2-x}Se$ NCs-in-Nafion Film. Since the most prominent plasmon tuning was achieved with the $Cu_{2-x}Se$ NCs-in-Nafion based electrode, we carefully characterized this sample by means of XPS in order to get an insight in the processes occurring during the redox reactions, and in particular to analyze the oxidation states of the main elements in the system before and after plasmon damping/restoring. For the analysis, as prepared electrodes were taken without lifting off the films or extracting the NCs. The signal from NCs in the films was remarkably strong making its quantification straightforward. As reference samples we used bare $Cu_{2-x}Se$ NCs deposited directly from their dispersion and pure Nafion film. In all samples containing the NCs Cu^{+} and Se^{2-} were detected (Figure 7). A closer look at the Cu 2p range (deconvolution of only one part of the doublet is shown in panel a for better readability of the figure) reveals that the 2p feature contains an obvious shoulder/asymmetry (denoted as "B") that matches in energy Cu(II) (shifted ∼0.5 eV toward higher binding energies from the main peak denoted "A"), even though no Cu(II) satellites are observed in the spectra. This line shape is rather the same for all three NC samples, but in both NCs-in-Nafion films (reduced and oxidized) it is shifted by 0.3 eV toward higher energies with respect to the pure NC reference. It is unlikely that this is due to the charging of the NCs in Nafion during the photoemission measurement, because (i) the Nafion is a rather conductive material and (ii) there was no indication of charging in the XPS spectra of NC ligands (C 1s, not shown). Generally, the higher binding energy means more positive charge in a probed species. Furthermore, the same trend is observed for the Se 3d core level. These spectra contain two contributions with the same shifts for all three samples, as for the Cu peak as well as for Se 3p peak, with no feature of oxidized selenium around 59 eV being present.[19] The additional component with 0.5−1.0 eV higher binding energy with respect to the main XPS peak is often observed for NCs and mostly assigned to the surface atoms, which are in a different chemical environment than the "bulk" ones.[42−44] In the Se 3p range also the S 2p contribution of the ligand (dodecanethiol) bound to the NC surface is found at 162−163 eV (Figure 7b). Interestingly, the S-related feature of Nafion at 170 eV disappears in the spectra of composites. This can be related to the coordination/binding of the Nafion's sulfur to the NC surface, because we also noticed an increase of the relative intensity of the S^{2-} doublet at 162−163 eV (Figure 7b). In addition, we observed that the F 1s feature of Nafion (not shown) shifts to lower binding energies in the composite with the NCs, which can be a result of the polymer carrying a more negative charge, as compared with the pure polymer.

Basically, the XPS analysis does not reveal any significant changes in the oxidation states and chemical environment of the main elements in the system before and after the reduction (damping of the LSPR). This means that the plasmon modulation is based solely on the charge injection/withdrawal mechanism. Here we note that in our approach we started with as-prepared nanoparticles with a large number of vacancies avoiding their additional oxidation which might be accompanied by a partial decomposition of the material. Furthermore, in such vacant NCs there are no extra Cu species present which can potentially be incorporated into the particles upon their reduction. On the basis of our observations of optical absorption changes in the system upon applying potential we can attribute the resulting plasmon tuning to the electron injection into the valence band of the $Cu_{2-x}Se$ NCs during their reduction with subsequent withdrawal by following oxidation, as schematized in Figure 8.

CONCLUSIONS

We introduced an electrochemical method of tuning the LSPR of degeneratively doped copper chalcogenide NCs. A combination of cyclic voltammetry and chronoamperometry techniques with absorption spectroscopy directly *in situ* allowed us to monitor optical changes straightaway during charging/discharging of $Cu_{2-x}Se$ and CuS NCs embedded in a transparent ionomer Nafion film. Even though both these materials exhibit an intensive LSPR band in the NIR spectral region, its behavior upon sweeping the potential was found to be different. In particular, whereas in the case of $Cu_{2-x}Se$ NCs based sample we achieved a complete and reversible plasmon damping followed by its regeneration during reduction and oxidation of the NCs, respectively, the LSPR of CuS NCs was much more stable under experimental conditions and exhibited only subtle changes in its position and intensity resembling the behavior of noble metal nanoparticles. XPS analysis of the $Cu_{2-x}Se$ NCs-in-Nafion sample did not reveal any prominent

DOI: 10.1021/acs.jpcc.7b05334
J. Phys. Chem. C 2017, 121, 18244−18253

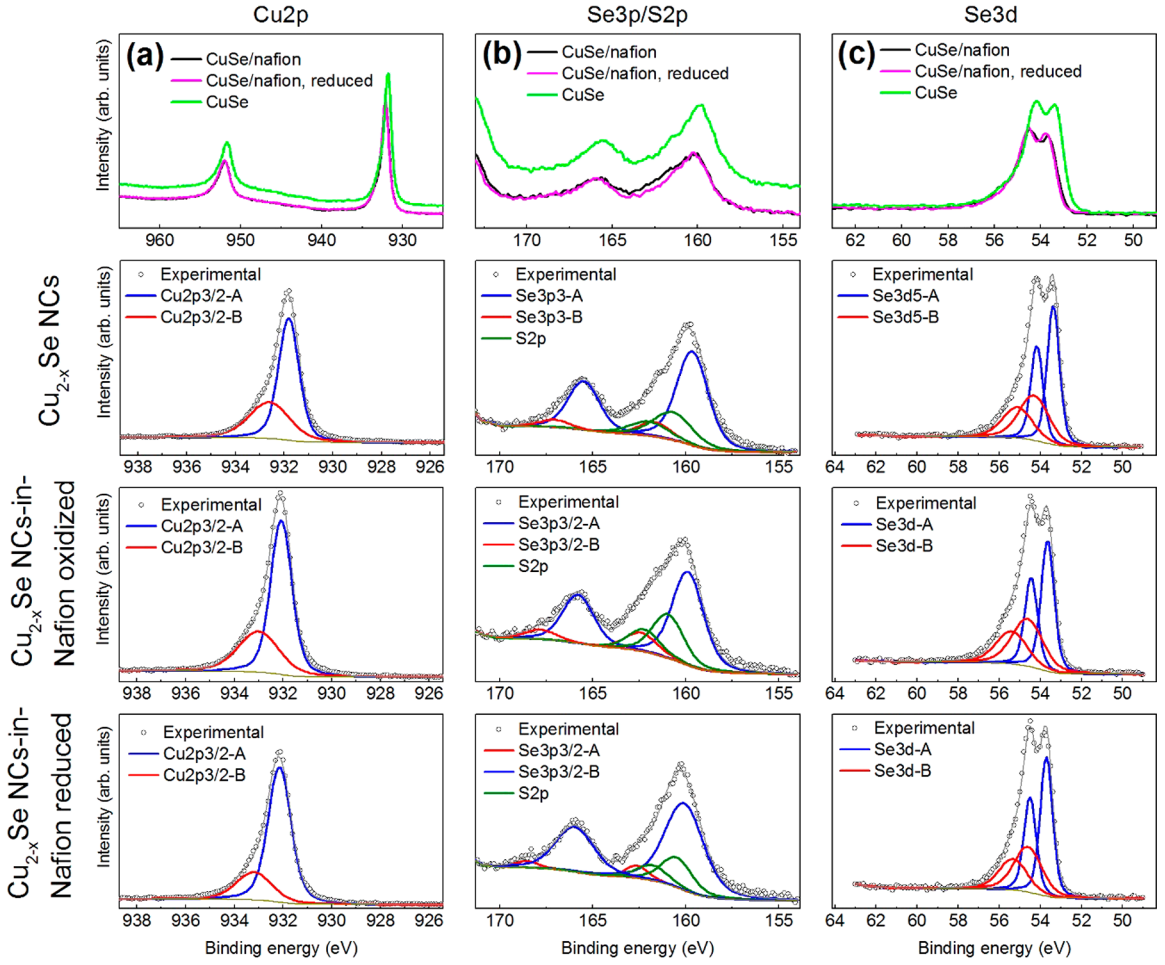

Figure 7. XPS scans of Cu $2p_{3/2}$ (panel a), as well as Se 3p and S 2p (panel b) and Se 3d (panel c) peaks of the $Cu_{2-x}Se$ NCs and the $Cu_{2-x}Se$ NCs-in-Nafion composites before and after reduction. Below in each panel are corresponding fits of the experimental peaks.

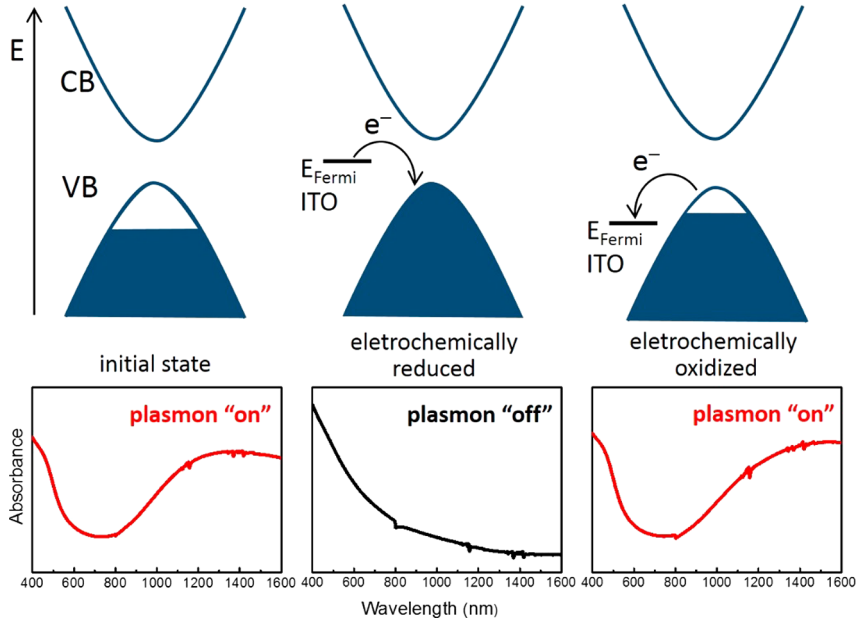

Figure 8. Schematized band gap structure of $Cu_{2-x}Se$ NCs proposed for the different stages of the LSPR electrochemical modulation with corresponding optical absorption spectra.

changes in oxidation states of the main elements before and after charging. This allows us to assign changes in absorption solely to electron injection/extraction processes leading to extinguishing and regeneration of free holes present in as-

DOI: 10.1021/acs.jpcc.7b05334
J. Phys. Chem. C 2017, 121, 18244−18253

synthesized NCs. We believe that our findings pave the way to several important applications of self-doped NIR plasmonic copper chalcogenide nanomaterials in the form of solid state films in photovoltaics, light filtering, electromagnetic filed-enhanced light emission, *etc.*

AUTHOR INFORMATION

Corresponding Author

*(V.L.) E-mail: vladimir.lesnyak@chemie.tu-dresden.de.

ORCID

Nikolai Gaponik: 0000-0002-8827-2881

Vladimir Lesnyak: 0000-0002-2480-8755

Notes

The authors declare no competing financial interest.

ACKNOWLEDGMENTS

V.B.L. acknowledges the short term fellowship funded by the DAAD Germany (short research stay grant ALERG) and the fellowship CONICET (grant Beca Interna Doctoral). We are grateful to Danny Haubold (TU Dresden) for TEM imaging. V.M.D. and D.R.T.Z. acknowledge the Volkswagen Foundation (Project No. 90366) for support. This work was supported by the German Research Foundation (DFG) under Project LE 3877/1-1.

REFERENCES

(1) Zhao, Y.; Burda, C. Development of Plasmonic Semiconductor Nanomaterials with Copper Chalcogenides for a Future with Sustainable Energy Materials. *Energy Environ. Sci.* **2012**, *5*, 5564−5576.

(2) Comin, A.; Manna, L. New Materials for Tunable Plasmonic Colloidal Nanocrystals. *Chem. Soc. Rev.* **2014**, *43*, 3957−3975.

(3) Mattox, T. M.; Ye, X.; Manthiram, K.; Schuck, P. J.; Alivisatos, A. P.; Urban, J. J. Chemical Control of Plasmons in Metal Chalcogenide and Metal Oxide Nanostructures. *Adv. Mater.* **2015**, *27*, 5830−5837.

(4) Liu, X.; Swihart, M. T. Heavily-Doped Colloidal Semiconductor and Metal Oxide Nanocrystals: An Emerging New Class of Plasmonic Nanomaterials. *Chem. Soc. Rev.* **2014**, *43*, 3908−3920.

(5) Faucheaux, J. A.; Stanton, A. L. D.; Jain, P. K. Plasmon Resonances of Semiconductor Nanocrystals: Physical Principles and New Opportunities. *J. Phys. Chem. Lett.* **2014**, *5*, 976−985.

(6) Kriegel, I.; Scotognella, F.; Manna, L. Plasmonic Doped Semiconductor Nanocrystals: Properties, Fabrication, Applications and Perspectives. *Phys. Rep.* **2017**, *674*, 1−52.

(7) Zhao, Y.; Pan, H.; Lou, Y.; Qiu, X.; Zhu, J.; Burda, C. Plasmonic $Cu_{2-x}S$ Nanocrystals: Optical and Structural Properties of Copper-Deficient Copper(I) Sulfides. *J. Am. Chem. Soc.* **2009**, *131*, 4253−4261.

(8) Luther, J. M.; Jain, P. K.; Ewers, T.; Alivisatos, A. P. Localized Surface Plasmon Resonances Arising from Free Carriers in Doped Quantum Dots. *Nat. Mater.* **2011**, *10*, 361−366.

(9) Saldanha, P. L.; Brescia, R.; Prato, M.; Li, H.; Povia, M.; Manna, L.; Lesnyak, V. Generalized One-Pot Synthesis of Copper Sulfide, Selenide-Sulfide, and Telluride-Sulfide Nanoparticles. *Chem. Mater.* **2014**, *26*, 1442−1449.

(10) Kriegel, I.; Jiang, C.; Rodríguez-Fernández, J.; Schaller, R. D.; Talapin, D. V.; da Como, E.; Feldmann, J. Tuning the Excitonic and Plasmonic Properties of Copper Chalcogenide Nanocrystals. *J. Am. Chem. Soc.* **2012**, *134*, 1583−1590.

(11) Dorfs, D.; Härtling, T.; Miszta, K.; Bigall, N. C.; Kim, M. R.; Genovese, A.; Falqui, A.; Povia, M.; Manna, L. Reversible Tunability of the Near-Infrared Valence Band Plasmon Resonance in $Cu_{2-x}Se$ Nanocrystals. *J. Am. Chem. Soc.* **2011**, *133*, 11175−11180.

(12) Lesnyak, V.; Brescia, R.; Messina, G. C.; Manna, L. Cu Vacancies Boost Cation Exchange Reactions in Copper Selenide Nanocrystals. *J. Am. Chem. Soc.* **2015**, *137*, 9315−9323.

(13) Lesnyak, V.; George, C.; Genovese, A.; Prato, M.; Casu, A.; Ayyappan, S.; Scarpellini, A.; Manna, L. Alloyed Copper Chalcogenide Nanoplatelets via Partial Cation Exchange Reactions. *ACS Nano* **2014**, *8*, 8407−8418.

(14) Li, W.; Zamani, R.; Rivera Gil, P.; Pelaz, B.; Ibáñez, M.; Cadavid, D.; Shavel, A.; Alvarez-Puebla, R. A.; Parak, W. J.; Arbiol, J.; Cabot, A. CuTe Nanocrystals: Shape and Size Control, Plasmonic Properties, and Use as SERS Probes and Photothermal Agents. *J. Am. Chem. Soc.* **2013**, *135*, 7098−7101.

(15) Xie, Y.; Carbone, L.; Nobile, C.; Grillo, V.; D'Agostino, S.; Della Sala, F.; Giannini, C.; Altamura, D.; Oelsner, C.; Kryschi, C.; Cozzoli, P. D. Metallic-Like Stoichiometric Copper Sulfide Nanocrystals: Phase- and Shape-Selective Synthesis, Near-Infrared Surface Plasmon Resonance Properties, and Their Modeling. *ACS Nano* **2013**, *7*, 7352−7369.

(16) Xie, Y.; Riedinger, A.; Prato, M.; Casu, A.; Genovese, A.; Guardia, P.; Sottini, S.; Sangregorio, C.; Miszta, K.; Ghosh, S.; Pellegrino, T.; Manna, L. Copper Sulfide Nanocrystals with Tunable Composition by Reduction of Covellite Nanocrystals with Cu^+ Ions. *J. Am. Chem. Soc.* **2013**, *135*, 17630−17637.

(17) Vikulov, S.; Di Stasio, F.; Ceseracciu, L.; Saldanha, P. L.; Scarpellini, A.; Dang, Z.; Krahne, R.; Manna, L.; Lesnyak, V. Fully Solution-Processed Conductive Films Based on Colloidal Copper Selenide Nanosheets for Flexible Electronics. *Adv. Funct. Mater.* **2016**, *26*, 3670−3677.

(18) Jain, P. K.; Manthiram, K.; Engel, J. H.; White, S. L.; Faucheaux, J. A.; Alivisatos, A. P. Doped Nanocrystals as Plasmonic Probes of Redox Chemistry. *Angew. Chem., Int. Ed.* **2013**, *52*, 13671−13675.

(19) Riha, S. C.; Johnson, D. C.; Prieto, A. L. Cu_2Se Nanoparticles with Tunable Electronic Properties Due to a Controlled Solid-State Phase Transition Driven by Copper Oxidation and Cationic Conduction. *J. Am. Chem. Soc.* **2011**, *133*, 1383−1390.

(20) Li, W.; Zamani, R.; Ibáñez, M.; Cadavid, D.; Shavel, A.; Morante, J. R.; Arbiol, J.; Cabot, A. Metal Ions to Control the Morphology of Semiconductor Nanoparticles: Copper Selenide Nanocubes. *J. Am. Chem. Soc.* **2013**, *135*, 4664−4667.

(21) Kriegel, I.; Rodríguez-Fernández, J.; Wisnet, A.; Zhang, H.; Waurisch, C.; Eychmüller, A.; Dubavik, A.; Govorov, A. O.; Feldmann, J. Shedding Light on Vacancy-Doped Copper Chalcogenides: Shape-Controlled Synthesis, Optical Properties, and Modeling of Copper Telluride Nanocrystals with Near-Infrared Plasmon Resonances. *ACS Nano* **2013**, *7*, 4367−4377.

(22) Hsu, S.-W.; On, K.; Tao, A. R. Localized Surface Plasmon Resonances of Anisotropic Semiconductor Nanocrystals. *J. Am. Chem. Soc.* **2011**, *133*, 19072−19075.

(23) Hsu, S.-W.; Bryks, W.; Tao, A. R. Effects of Carrier Density and Shape on the Localized Surface Plasmon Resonances of $Cu_{2-x}S$ Nanodisks. *Chem. Mater.* **2012**, *24*, 3765−3771.

(24) Liu, X.; Wang, X.; Zhou, B.; Law, W.-C.; Cartwright, A. N.; Swihart, M. T. Size-Controlled Synthesis of $Cu_{2-x}E$ (E = S, Se) Nanocrystals with Strong Tunable Near-Infrared Localized Surface Plasmon Resonance and High Conductivity in Thin Films. *Adv. Funct. Mater.* **2013**, *23*, 1256−1264.

(25) Balitskii, O. A.; Sytnyk, M.; Stangl, J.; Primetzhofer, D.; Groiss, H.; Heiss, W. Tuning the Localized Surface Plasmon Resonance in $Cu_{2-x}Se$ Nanocrystals by Postsynthetic Ligand Exchange. *ACS Appl. Mater. Interfaces* **2014**, *6*, 17770−17775.

(26) Haram, S. K.; Quinn, B. M.; Bard, A. J. Electrochemistry of CdS Nanoparticles: A Correlation between Optical and Electrochemical Band Gaps. *J. Am. Chem. Soc.* **2001**, *123*, 8860−8861.

(27) Ma, X.; Mews, A.; Kipp, T. Determination of Electronic Energy Levels in Type-II CdTe-Core/CdSe-Shell and CdSe-Core/CdTe-Shell Nanocrystals by Cyclic Voltammetry and Optical Spectroscopy. *J. Phys. Chem. C* **2013**, *117*, 16698−16708.

(28) Amelia, M.; Lincheneau, C.; Silvi, S.; Credi, A. Electrochemical Properties of CdSe and CdTe Quantum Dots. *Chem. Soc. Rev.* **2012**, *41*, 5728−5743.

(29) Osipovich, N. P.; Poznyak, S. K.; Lesnyak, V.; Gaponik, N. Cyclic Voltammetry as a Sensitive Method for in Situ Probing of

DOI: 10.1021/acs.jpcc.7b05334
J. Phys. Chem. C 2017, 121, 18244−18253

Chemical Transformations in Quantum Dots. *Phys. Chem. Chem. Phys.* **2016**, *18*, 10355−10361.
(30) Ingole, P. P.; Lesnyak, V.; Tatikondewar, L.; Leubner, S.; Gaponik, N.; Kshirsagar, A.; Eychmüller, A. Probing Absolute Electronic Energy Levels in Hg-Doped CdTe Semiconductor Nanocrystals by Electrochemistry and Density Functional Theory. *ChemPhysChem* **2016**, *17*, 244−252.
(31) Poznyak, S. K.; Osipovich, N. P.; Shavel, A.; Talapin, D. V.; Gao, M.; Eychmüller, A.; Gaponik, N. Size-Dependent Electrochemical Behavior of Thiol-Capped CdTe Nanocrystals in Aqueous Solution. *J. Phys. Chem. B* **2005**, *109*, 1094−1100.
(32) Bard, A. J.; Faulkner, L. R. *Electrochemical Methods: Fundamentals and Applications*, 2nd ed.; John Wiley & Sons, Inc.: 2001; p 864.
(33) Park, J.-E.; Kim, J.; Nam, J.-M. Emerging Plasmonic Nanostructures for Controlling and Enhancing Photoluminescence. *Chem. Sci.* **2017**, *8*, 4696−4704.
(34) Dong, J.; Zhang, Z.; Zheng, H.; Sun, M. Recent Progress on Plasmon-Enhanced Fluorescence. *Nanophotonics* **2015**, *4*, 472−490.
(35) Zhou, N.; Lopez-Puente, V.; Wang, Q.; Polavarapu, L.; Pastoriza-Santos, I.; Xu, Q.-H. Plasmon-Enhanced Light Harvesting: Applications in Enhanced Photocatalysis, Photodynamic Therapy and Photovoltaics. *RSC Adv.* **2015**, *5*, 29076−29097.
(36) Inzelt, G. Pseudo-Reference Electrodes. In *Handbook of Reference Electrodes*, Inzelt, G.; Lewenstam, A.; Scholz, F., Eds.; Springer Berlin Heidelberg: Berlin and Heidelberg, Germany, 2013; pp 331−332.
(37) Mauritz, K. A.; Moore, R. B. State of Understanding of Nafion. *Chem. Rev.* **2004**, *104*, 4535−4586.
(38) Kusoglu, A.; Weber, A. Z. New Insights into Perfluorinated Sulfonic-Acid Ionomers. *Chem. Rev.* **2017**, *117*, 987−1104.
(39) Jalas, D.; Shao, L. H.; Canchi, R.; Okuma, T.; Lang, S.; Petrov, A.; Weissmüller, J.; Eich, M. Electrochemical Tuning of the Optical Properties of Nanoporous Gold. *Sci. Rep.* **2017**, *7*, 44139.
(40) Brown, A. M.; Sheldon, M. T.; Atwater, H. A. Electrochemical Tuning of the Dielectric Function of Au Nanoparticles. *ACS Photonics* **2015**, *2*, 459−464.
(41) Kalanur, S. S.; Seo, H. Tuning Plasmonic Properties of CuS Thin Films via Valence Band Filling. *RSC Adv.* **2017**, *7*, 11118−11122.
(42) Borchert, H.; Talapin, D. V.; McGinley, C.; Adam, S.; Lobo, A.; de Castro, A. R. B.; Möller, T.; Weller, H. High Resolution Photoemission Study of CdSe and CdSe/ZnS Core-Shell Nanocrystals. *J. Chem. Phys.* **2003**, *119*, 1800−1807.
(43) Sayevich, V.; Guhrenz, C.; Dzhagan, V. M.; Sin, M.; Werheid, M.; Cai, B.; Borchardt, L.; Widmer, J.; Zahn, D. R. T.; Brunner, E.; Lesnyak, V.; Gaponik, N.; Eychmüller, A. Hybrid N-Butylamine-Based Ligands for Switching the Colloidal Solubility and Regimentation of Inorganic-Capped Nanocrystals. *ACS Nano* **2017**, *11*, 1559−1571.
(44) Raevskaya, A.; Rosovik, O.; Kozytskiy, A.; Stroyuk, O.; Dzhagan, V.; Zahn, D. R. T. Non-Stoichiometric Cu-In-S@ZnS Nanoparticles Produced in Aqueous Solutions as Light Harvesters for Liquid-Junction Photoelectrochemical Solar Cells. *RSC Adv.* **2016**, *6*, 100145−100157.

DOI: 10.1021/acs.jpcc.7b05334
J. Phys. Chem. C 2017, 121, 18244−18253